A Mechanical Test Frame for Property Evaluations at Cryogenic Temperature

Daniel R. Merkel, Gayaneh Petrossian, Dustin Clelland, Kevin Simmons

Pacific Northwest National Laboratory
Richland, WA 99352, USA

ABSTRACT

On-board storage of hydrogen fuel has been designated as a limiting factor in the advancement of fuel cell technologies in the automotive industry. The use of cryo-compressed Type III pressure vessels presents one option to overcome this barrier. These multi-material vessels will be expected to perform at high pressure and extreme low temperatures, which creates a complex engineering design challenge. Many materials exhibit highly temperature-dependent properties, which must be considered for the efficient design of cryo-compressed pressure vessels. Complicating this issue, mechanical property data at cryogenic temperatures is sparse. This technical paper provides a description of a test apparatus commissioned specifically to help address this shortcoming. A mechanical test frame was retrofitted with a continuous flow cryostat capable to evaluate various mechanical properties throughout a broad temperature range of 25 °C to -269 °C with a load limit of 10 kN. An investigation of the thermomechanical properties of an epoxy resin was carried out as a demonstration.

Corresponding author: Daniel R. Merkel (daniel.merkel@pnnl.gov)

1. INTRODUCTION

The Department of Energy Fuel Cell Technology Office has designated the on-board storage of hydrogen fuel as a limiting factor in the advancement of fuel cell technologies in the automotive industry[1]. The key challenge in this regard is overcoming the low energy density of hydrogen at ambient temperature and pressure. One approach to improve this metric is cryo-compressed hydrogen storage vessels[2]–[4]. Target design specifications for such vessels are pressures up to 700 bar and temperatures as low as -253 °C[5]. Simultaneously, on-board cryo-compressed vessels must also meet weight constraints associated with automotive components to maintain vehicle efficiency[6]. Given these criteria, recent analyses deemed Type III pressure vessels to be of particular interest for this design challenge[7], [8].

Type III pressure vessels are commonly used in industrial applications for gas storage when low system weight is of importance[6], [7]. The vessels represent a multimaterial system consisting of a metal tank liner with a filament wound carbon fiber composite overwrap. This combination of dissimilar materials provides an efficient means to contain high pressure while conserving weight[7]. Pressure vessel designers rely on available material properties data to design efficient vessels; however, this data is generally limited at extreme low temperatures. As a result, designers must rely on best-estimates interpolated from just a few existing data points. This is especially problematic considering that the available data is reliable only for industrially relevant materials and has largely been collected at the boil-off temperatures of cryogenic liquids, *i.e.* -269 °C (helium) and -196 °C (nitrogen) [9]–[11].

This technical paper documents the recent development of a cryogenic test system commissioned specifically to address the current needs of cryo-compressed vessel designers. The system is designed to evaluate mechanical properties in a continuous temperature range of -269 °C to 25 °C at loads up to 10 kN. This paper provides an overview of the design and operation of the instrument. The tensile properties of a generic epoxy resin were investigated at -233 °C, -125 °C, and 25 °C. Techniques for geometric design of tensile specimens and fixturing methods to overcome complications associated with cryogenic testing are described.

2. Experimental Methods

2.1 Cryogenic Mechanical Test Apparatus

Mechanical test specimens were cooled to the desired temperature in a continuous flow cryostat purpose-built for mechanical testing (STVP-200, Janis Research Co., Woburn, MA). The cryostat was mounted on a 222 kN (50,000 lbf) limit mechanical test frame (MTS, Eden Prairie, MN) modified to accommodate the cryostat. The hydraulic actuator and main load train were removed from the frame to accommodate the cryostat. The bottom platen of the frame was lowered and fitted with an adapting plate to allow fixturing to the cryostat. The upper crosshead was fitted with a second adapting plate such that a servoelectric actuator (10K Servo Creep Controller, Interactive Instruments, Scotia, NY) could be mounted with the main load train extending from the actuator down through a center hole in the crosshead. A 44.5 kN (10,000 lbf) load cell was mounted directly to the actuator in-line with the main load train. The apparatus is shown in Figure 1.

The cryostat consisted of an external mechanical load frame (labeled in Figure 1a), an insulating vacuum jacket, and an internal mechanical load frame (shown in Figure 1b). The external frame remained permanently fixtured to the insulating jacket; the internal frame was removed from the cryostat between each test to remove and replace test specimens. A load rod extended from the test space of the internal frame through the top plate of the cryostat, supplying a direct mechanical linkage between the test specimen inside the cryostat to the main load train of the test frame. The load rod was linked to the load train by a pin-clevis type linkage, which allowed the cryostat to be mounted/removed from the test frame rapidly between tests. Zero-load conditions were maintained on the test specimen during mounting/removal of the cryostat using a collar limiting vertical motion of the load rod, along with button-head style specimen grips designed to prevent compression of the test specimen. The cryostat was rated for a maximum load of 10 kN (2,250 lbf.).

Tensile load was applied to test specimens via the load rod linked to the servoelectric actuator. The reaction force was carried through the bottom specimen grip, transferred to the internal load frame through the bottom plate, then transferred to the external load frame by the top plate. During a tensile test, the internal frame and external frame assumed compressive and tensile states, respectively.

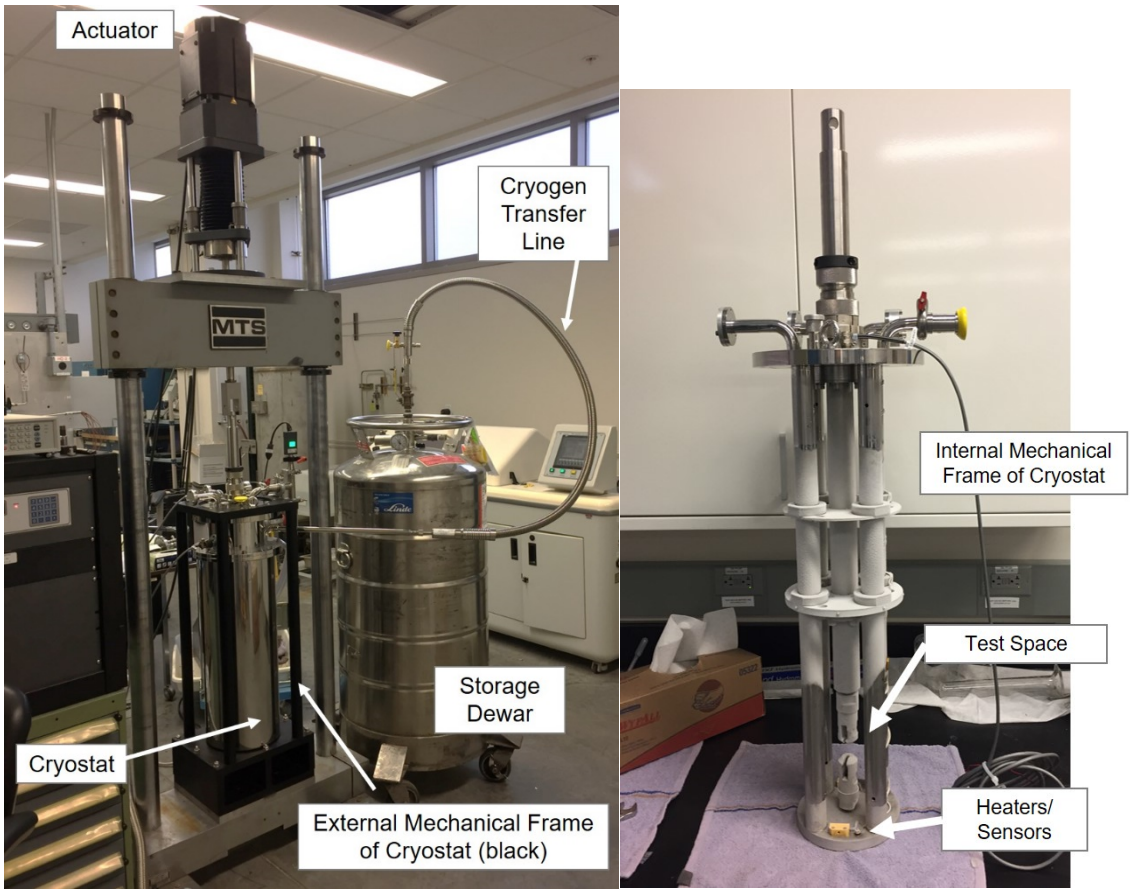

Figure 1. (a) Mechanical testing cryostat assembled in MTS load frame with cryogen storage tank. (b) Internal mechanical frame of the cryostat.

2.2 Temperature control

Temperature was manipulated by coordination of manually controlled cryogen flow and digital PID controlled heating elements. Cooling was achieved by the continuous flow of liquid cryogen from a cryogen storage dewar to the cryostat via a purpose-built vacuum insulated transfer line (FHT-ST, Janis Research Co.). The insulating vacuum jacket of the transfer line was evacuated to 10^{-4} Torr using a turbomolecular vacuum pump. Either liquid helium or liquid nitrogen was used as the cryogen with minimum temperatures corresponding to the boiling points of each species, *i.e.* -269 °C and -196 °C, respectively. Cryogen flow into the cryostat was encouraged by creating a pressure differential between the cryogen storage dewar and the sample space of cryostat. In the case of liquid helium, slight vacuum was generated in the sample space of the cryostat using a mechanical vacuum pump. In the case of liquid nitrogen, pressurized nitrogen gas was used to maintain 27.6 kPa (4 psi) in the storage dewar while the sample space of the cryostat was maintained at ambient pressure. A manual valve in the transfer line was used to control the flow rate of cryogen. Liquid cryogen flowed through the transfer line to a small compartment at the bottom of the cryostat where the cryogen was vaporized to gas phase. The cryogen gas then flowed into the sample space to cool the test specimen and internal load frame.

Silicon diode heaters/temperatures sensors were mounted in the cryostat in two spaces. Two heaters/sensors mounted in the vaporizer space controlled the rate of vaporization of liquid cryogen as it flowed into the cryostat. Another two heaters/sensors mounted on the bottom plate of the internal frame of the cryostat near the test specimen controlled the temperature of the specimen. The temperatures of the vaporizer and sample spaces were controlled independently by a temperature controller (Model 336, Lake Shore Cryotronics, Westerville, OH). Typically, the temperature of the vaporizer space was set to 2 °C less than that of the sample space.

2.3 Tensile Geometry

Two specimen geometries were explored for tensile testing. First, the ASTM D638 Type II specimen, shown Figure 2a, was explored. Several issues were discovered during preliminary testing. First, the large material volume and surface area proved problematic at lower temperatures due to defect sensitivity of the epoxy. Rarely could such large specimens be made without significant defects such as air bubbles occurring in the narrow section of the specimen. When defects were influential, tensile fracture always initiated from a corner of the square cross-section. Additionally, gripping the flat-type geometry using self-tightening wedge grips at sub-ambient temperatures was often complicated by ice formation on the grip surface or stress risers developing outside the narrow section of the specimen due to gripping. Complications also arose due to thermal contraction during cooling, which imposed significant and undesirable tension on the specimen during test setup.

To mitigate these issues, a sub-size ASTM E8 cylindrical geometry was adopted, shown in Figure 2. The small volume and circular cross-section reduced the number of defects in each specimen. This geometry also allowed a button-head style gripping method that was not complicated by icing or stress risers outside the narrow section. This gripping technique also eliminated issues related to thermal contraction during cooling. Test specimens could be setup in the grips and instrumented with an extensometer without imposing a tensile state. Thus, the test assembly could be cooled to extreme low temperatures without inducing an undesired tensile state in the specimen. Fixturing grips were designed accordingly with special consideration of mechanical properties throughout the temperature of 0 °C to 25 °C. Nitronic 60 steel was chosen as an alternative to 300-series stainless steel to minimize mass of the grip while maintaining ductility at extreme low temperatures.

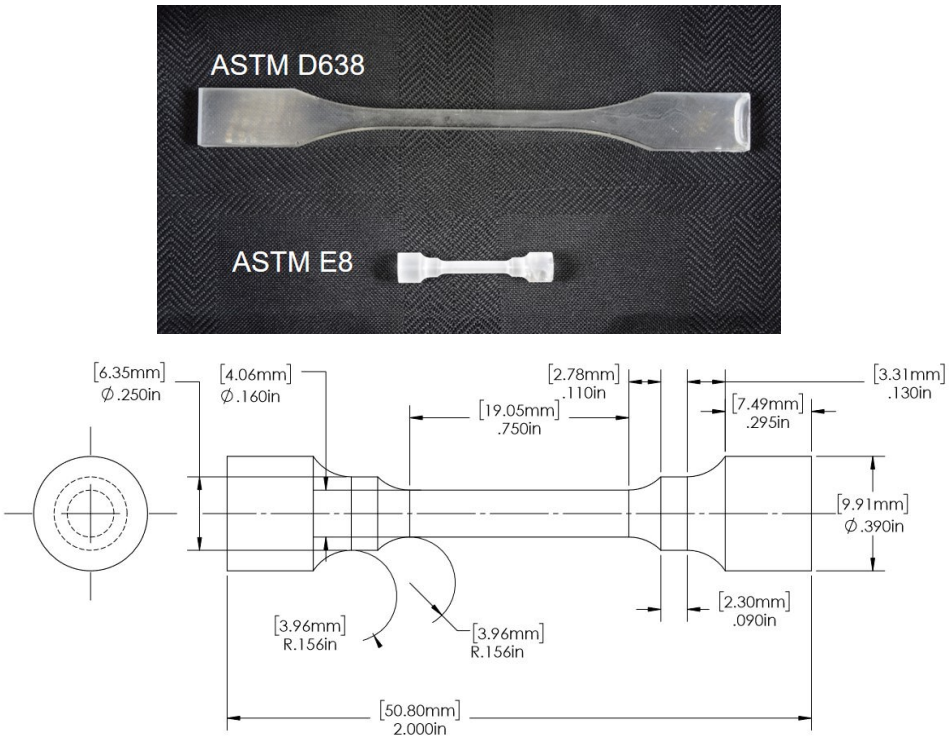

Figure 2. Tensile geometry for ASTM D638 Type II and sub-size E8.

2.4 Tensile Property Evaluation

Tensile properties were evaluated at a constant machine rate of 1.91 mm/min (0.075 in/min). A mechanical extensometer (3442-0064-025T-LHT, Epsilon Technology Corp, Jackson, WY) rated for minimum temperatures of -270 °C was used to evaluated strain during each tensile test. Tensile modulus was determined by linear fit of stress-strain curves in the initial portion (typically less than 1 % strain) of each test.

2.5 Materials

Commercially available bisphenol-A epichlorohydrin epoxy resin (EPON resin 828, Hexion Specialty Chemicals, Columbus, OH) having a density of 1.16 g/ml and a viscosity of 110-150 P at 25 °C was used as the base resin. Technical grade triethylenetetraamine (TETA) curing agent was purchased from Sigma-Aldrich (St. Louis, MO) with 60 % purity and a molecular weight of 146.23 g/mol. A stoichiometric amount of TETA was added to the epoxy resin at 18.1 phr and the mixture was degassed under 30 in-Hg vacuum for approximately 5 minutes. Prior to mixing, the resin was heated at 60 °C for 30 minutes. The resin mixture was then poured into silicone rubber molds and cured overnight at room temperature. The partially cured samples were taken out of the molds and post-cured in the oven at 100 °C for 3h. The samples were then heated to 125 °C for 1h and quench cooled to room temperature to relieve internal stress due to curing.

Differential scanning calorimetry (DSC Q2000, TA instruments, New Castle, DE) was used to establish the cure schedule and confirm full cure. A small amount (approximately 5 mg) of cured

epoxy was cut and packaged in a closed lid aluminum Tzero DSC pan. Samples were heated to 200 °C at 10 °C/min, kept for 5 minutes to reach equilibrium, then cooled down to 25 °C at 10 °C/min, kept for another 5 minutes, and finally heated to 200 °C again to confirm the full curing of the sample.

Dynamic mechanical analysis (DMA Q800, TA instruments) was performed to better understand the thermomechanical behavior of the resin mixture. All measurements were performed using a heating rate of 2 °C/min starting from -140 °C. Dual cantilever grips were used at a fixed strain, with an amplitude of 5 μm and an oscillation frequency of 1 Hz. TA Universal Analysis software was used for analyzing the DSC and DMA data.

3. Results

3.1 Thermal and Dynamic Properties

A comprehensive differential scanning calorimetry study was carried out, both isothermal and dynamic, in order to establish a cure schedule for the mixture and eliminate any existing thermal stress. For the first step of the analysis, a mixture of the resin and curing agent was heated to a maximum temperature resulting in full cure without reaching the degradation temperature. The resin and the curing agent were mixed at room temperature and tested immediately afterwards. An exothermic curing peak was observed around 100 °C, as shown in Figure 3a. During cooling, a glass transition of 114 °C was recorded. Figure 3b demonstrates the DSC curve of the mixture after curing. No exothermic peaks were observed, which indicates the full curing of the sample. The glass transition was determined as the middle of the sloped region, which varies slightly during heating and cooling. The glass transition temperature noted during heating and cooling for were at 127 °C and 113 °C, respectively.

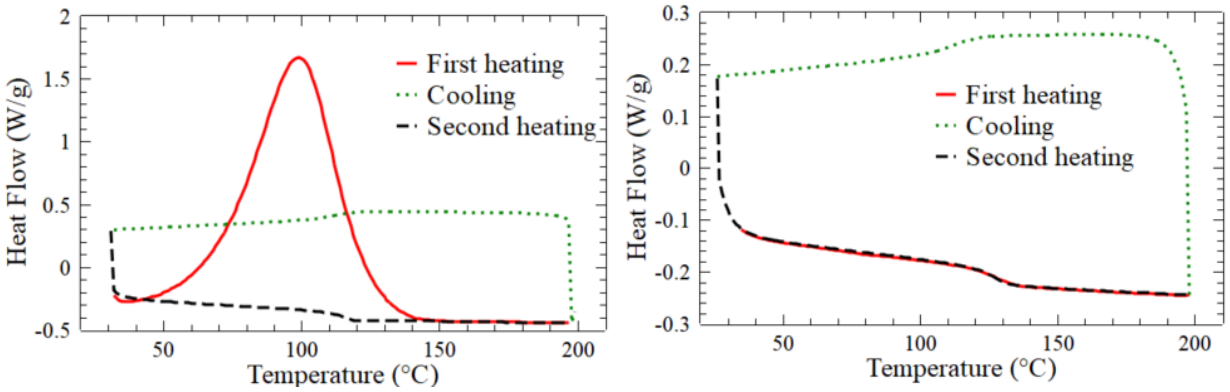

Figure 3. Differential scanning calorimetry (DSC) thermographs of (a) resin and curing agent immediately after mixing and (b) fully cured sample. Exothermic heat flow is oriented upward on the vertical axis.

Figure 4 shows the DMA curve for the fully cured epoxy. Three thermal transitions were observed, as indicated by the loss modulus peaks at 120 °C, 46 °C, and -42 °C. The high temperature peak at 120 °C corresponds to the glass transition or α-transition. Above this point, the samples were rubbery due to increased mobility of the molecular network chain. This

transition appeared at a slightly higher temperature when evaluated by DSC owing to the significantly faster heating rate of 10 °C/min used in the DSC method. A subtle intermediate relaxation called the ω-transition was observed at 46 °C attributed to mobility of larger segment of the network structure[12]. Finally, the β-transition was observed at -42 °C representing the local and short segment motion of the chains. Below this temperature, the sample was significantly more brittle.

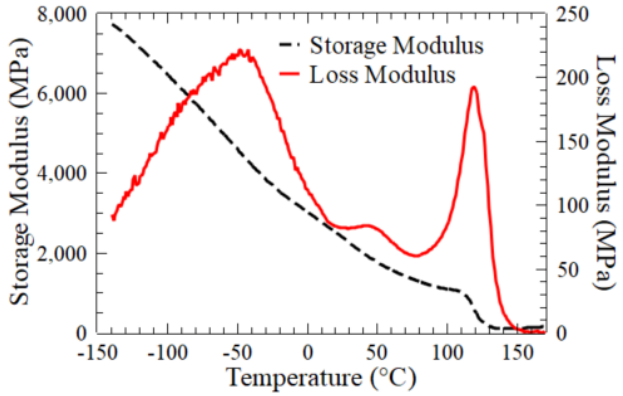

Figure 4. Dynamic mechanical analysis (DMA) of fully cured epoxy.

3.2 Tensile Properties

The cryostat mechanical test frame was used to evaluate tensile properties of epoxy specimens at a fixed crosshead rate. Tests were conducted at 25, -125, and -233 °C to examine the influence of temperature of tensile modulus. Stress-strain curves are shown in Figure 5 and tensile modulus is shown tabulated in Table 1. At 25 °C, the tensile response was approximately linear up to about 2 % strain. Continued deformation caused yielding as ductile deformation took place until failure. The tensile response at -125 °C and -233 °C were strictly brittle and linear to the point of failure. This transition from ductile to brittle behavior was consistent with DMA results, which showed significant thermal transition at -42°C. Likewise, tensile modulus increased as temperature decreased.

Tensile strength observed at low temperatures was significantly lower compared to the strength observed at 25 °C. Considering the brittle nature of failure, defect sensitivity appears to be a limiting factor causing premature failure. This is consistent with previous observations of epoxies at extreme low temperatures [13]. Additional stresses induced by the mechanical extensometer may also have played a role in limiting observable tensile strengths. These stresses would have been induced at the points where the extensometer arms attach to the specimen and result from a combination of the attachment method and extensometer weight. Typically, these influences are negligible compared to the strength of the material and are not expected to influence material performance. However, materials such as epoxy become increasingly brittle and sensitive to these influences at lower temperatures, making this a particularly difficult issue to resolve.

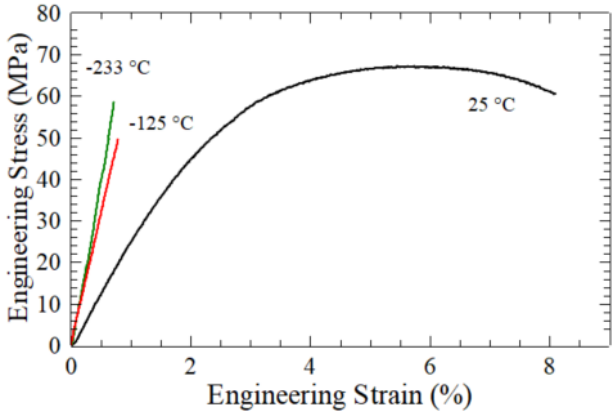

Figure 5. Representative tensile curves of epoxy at three temperatures.

Table 1. Tensile modulus of epoxy.

Temperature (°C)	Tensile Modulus (GPa) ± SD	Tensile Modulus (ksi) ± SD
25	2.76 ± 0.14 (*n*=6)	400 ± 21 (*n*=6)
-125	6.14 ± 0.26 (*n*=2)	890 ± 37 (*n*=2)
-233	8.29 (*n*=1)	1203 (*n*=1)

4. Conclusions

A mechanical test frame was retrofitted to accommodate a continuous flow liquid helium cryostat. The system was designed to evaluate mechanical properties at temperatures of -269 °C to 25 °C and loads up to 10 kN. A cylindrical geometry based on ASTM E8 was selected to minimize material defects, facilitate specimen gripping at cryogenic temperatures, and mitigate issues with thermal contraction of the specimen and/or instrument during cool-down.

Thermomechanical properties of an epoxy consisting of a bisphenol-A epichlorohydrin resin cured with TETA were studied. A curing schedule was established by DSC analysis of the epoxy mixture during and after cure. Thermal transitions at 120 °C, 46 °C, and -42 °C were observed by DMA, indicated by peaks of the loss modulus curve. Tensile properties were evaluated using the cryogenic mechanical test frame at three temperatures: 25 °C, -125 °C, and -233 °C. At 25 °C, epoxy deformed non-linearly with yielding beyond approximately 2% strain. The tensile response at -125 °C and -233 °C was linear with brittle failure. The transition from ductile to brittle behavior with temperature decrease agreed with the transition observed at -42 °C by DMA. Tensile modulus increased with decreasing temperature.

5. Acknowledgements

This work was fully supported by the U.S. Department of Energy (US DOE), Office of Energy Efficiency and Renewable Energy (EERE), Fuel Cell Technologies Office (FCTO) under Contract No. DE-AC05-76RL01830.

6. Disclaimers

The views and opinions of the authors expressed herein do not necessarily state or reflect those of the United States Government or any agency thereof. Neither the United States Government nor

any agency thereof, nor any of their employees, makes any warranty, expressed or implied, or assumes any legal liability or responsibility for the accuracy, completeness, or usefulness of any information, apparatus, product, or process disclosed, or represents that its use would not infringe privately owned rights.

7. References

[1] U.S. DRIVE Partnership, "Hydrogen Storage Tech Team Roadmap," 2017.

[2] J. Moreno-Blanco, G. Petitpas, F. Espinosa-Loza, F. Elizalde-Blancas, J. Martinez-Frias, and S. M. Aceves, "The storage performance of automotive cryo-compressed hydrogen vessels," *Int. J. Hydrogen Energy*, vol. 44, no. 31, pp. 16841–16851, 2019.

[3] D. J. Durbin and C. Malardier-Jugroot, "Review of hydrogen storage techniques for on board vehicle applications," *Int. J. Hydrogen Energy*, vol. 38, no. 34, pp. 14595–14617, 2013.

[4] H. Barthelemy, M. Weber, and F. Barbier, "Hydrogen storage: Recent improvements and industrial perspectives," *Int. J. Hydrogen Energy*, vol. 42, no. 11, pp. 7254–7262, 2017.

[5] R. K. Ahluwalia, J. K. Peng, H. S. Roh, T. Q. Hua, C. Houchins, and B. D. James, "Supercritical cryo-compressed hydrogen storage for fuel cell electric buses," *Int. J. Hydrogen Energy*, vol. 43, no. 22, pp. 10215–10231, 2018.

[6] S. Aceves, "Analytical and experimental evaluation of insulated pressure vessels for cryogenic hydrogen storage," *Int. J. Hydrogen Energy*, vol. 25, no. 11, pp. 1075–1085, Nov. 2000.

[7] J. H. S. Almeida, H. Faria, A. T. Marques, and S. C. Amico, "Load sharing ability of the liner in type III composite pressure vessels under internal pressure," *J. Reinf. Plast. Compos.*, vol. 33, no. 24, pp. 2274–2286, Dec. 2014.

[8] B. N. Nguyen, D. R. Merkel, K. I. Johnson, D. W. Gotthold, K. L. Simmons, and H. S. Roh, "Modeling the effects of loading scenario and thermal expansion coefficient on potential failure of cryo-compressed hydrogen vessels," *Int. J. Hydrogen Energy*, no. xxxx, Oct. 2019.

[9] B. Atli-Veltin, "Cryogenic composite fuel tanks: The mechanical performance of advanced composites at low temperatures," *2018 AIAA/ASCE/AHS/ASC Struct. Struct. Dyn. Mater. Conf.*, no. January, 2018.

[10] J. Schneider, M. Dyess, C. Hastings, J. Patterson, J. Noorda, and T. DeLay, "Lightweight Cryogenic Composit Over-wrapped Pressure Vessels (COPVS) for Launch Vehicle Applications," in *48th AIAA/ASME/ASCE/AHS/ASC Structures, Structural Dynamics, and Materials Conference*, 2007, no. April, pp. 1–19.

[11] T. K. DeLay, J. Patterson, J. Noorda, and J. Schneider, "Development of Cryogenic Composite Over-Wrapped Pressure Vessels (COPV's)," *SAMPE J.*, vol. 44, no. 3, 2008.

[12] R. Ramsdale-Capper and J. P. Foreman, "Internal antiplasticisation in highly crosslinked amine cured multifunctional epoxy resins," *Polymer (Guildf).*, vol. 146, pp. 321–330, 2018.

[13] R. P. Reed and J. D. McColskey, "NISTIR5024: Properties of Neat-Resin Systems," in *Composite Struts for SMES Plants*, NIST, 1994, pp. 17–200.